RSC Advances

ROYAL SOCIETY OF CHEMISTRY

www.rsc.org/advances

Graphical Abstract

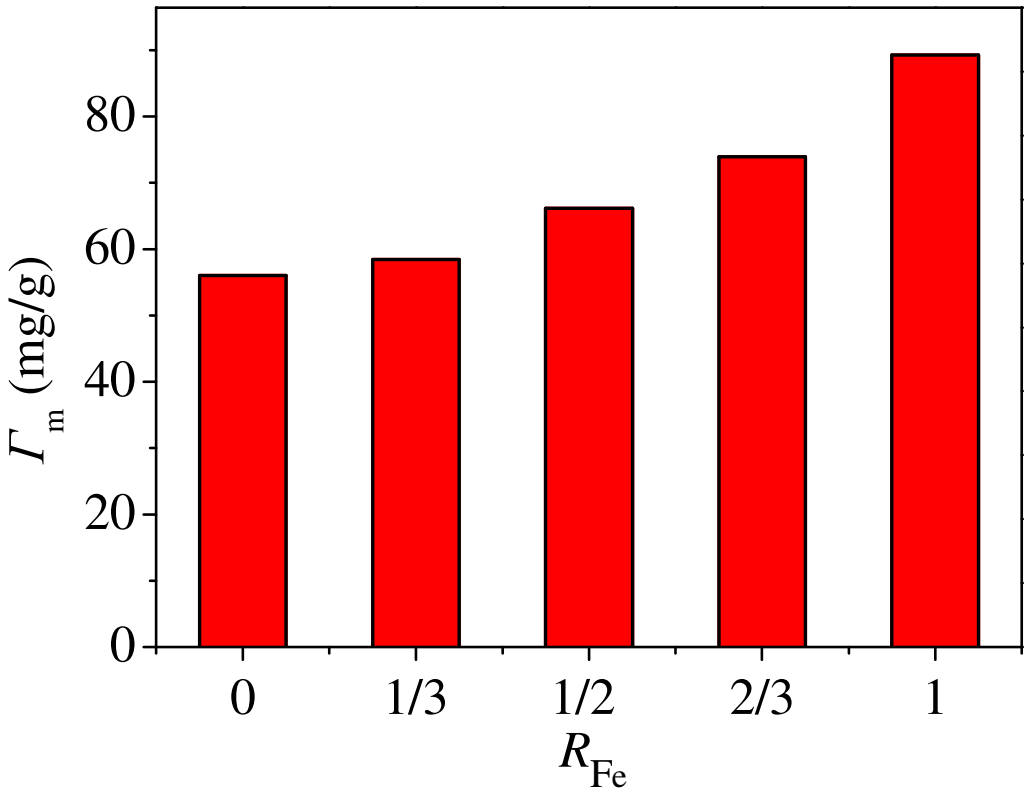

Mg–Al–Fe layered double hydroxides (LDHs) with a constant Mg/(Fe+Al) molar ratio but varying Fe/(Al+Fe) molar ratios (R_{Fe}) from 0–1 were synthesized by a mechanochemical method. Sorption of Cr(VI) on the LDHs in aqueous solution was investigated. With increasing Fe content in the LDHs, sorption capacity for Cr(VI) increased. The mechanochemical method can be used to synthesize LDH sorbents.

Sorption of Cr(VI) on Mg–Al–Fe Layered Double Hydroxides Synthesized by Mechanochemical Method †

Fengrong Zhang [a], Na Du [b], Haiping Li [c], Xuefeng Liang [d], Wanguo Hou [b] *

[a] *Environment Research Institute, Shandong University, Jinan 250199, P.R. China*

[b] *Key Laboratory of Colloid and Interface Chemistry (Ministry of Education), Shandong University, Jinan 250199, P.R. China*

[c] *National Engineering Technology Research Center for Colloidal Materials, Shandong University, Jinan 250199, P.R. China*

[d] *Agro-environmental protection institute, minstry of agriculture, Tianjin 300000, P.R. China*

* To whom correspondence should be addressed

Email: wghou@sdu.edu.cn

Tel: +86-0531-88564750

Fax: +86-0531-88564750

† Electronic supplementary information (ESI) available. See DOI: ??????

Abstract

Mg–Al–Fe layered double hydroxides (LDHs) with a constant $Mg^{2+}/(Fe^{3+}+Al^{3+})$ molar ratio but varying $Fe^{3+}/(Al^{3+}+Fe^{3+})$ molar ratios (R_{Fe}) from 0–1 were synthesized by a mechanochemical method. Sorption of Cr(VI) on the LDHs in aqueous solutions was investigated by a batch technique. The sorption process obeyed pseudo-second-order kinetics, and the sorption equilibrium could be well described with the Freundlich isotherm. The saturated sorption amount increased with increasing R_{Fe}, indicating that the replacement of Al by Fe in LDHs is favorable for Cr(VI) sorption. The mechanisms of Cr(VI) sorption included the intercalation of Cr(VI) oxyanions into the LDH gallery, and the surface complexation between dichromate anions and hydroxyl groups of the LDHs. The driving forces of Cr(VI) sorption on LDHs included physical binding (or electrostatic attraction) and chemical binding. The physically sorbed amount of Cr(VI) on the LDHs was almost independent of R_{Fe}, while the chemical sorbed amount obviously increased with increasing R_{Fe}. That is, the increase of R_{Fe} causes the chemical activity of surface sorption sites of the LDHs to increase, resulting in their sorption capacity for Cr(VI) increasing. In addition, the sorption capacity of the LDHs synthesized by the mechanochemical method is comparable with those of LDHs synthesized by coprecipitation and hydrothermal methods. Thus, Mg–Fe LDHs are promising sorbents for treating Cr(VI)-containing wastewater, and the mechanochemical method can be used to synthesize LDH sorbents.

Keywords: Layered double hydroxide; Mechanochemical method; Sorption; Cr(VI)

1. Introduction

The increasing worldwide contamination of freshwater systems with thousands of industrial and natural chemical compounds has become one of the key environmental problems facing humanity.[1] Hexavalent chromium (Cr(VI)) is a common heavy metal ion pollutant introduced into natural waters by the discharge of wastewaters from several industrial processes, such as electroplating, leather tanning, chromite beneficiation, metal finishing, and pigment manufacture.[2] Cr(VI), which exists in most aquatic environments as water soluble oxyanions ($HCrO_4^-$ or CrO_4^{2-}), is highly toxic and harmful to living organisms because of its carcinogenic and mutagenic properties.[3,4] Exposure to Cr(VI) in drinking water increases the risk of bladder, liver, kidney, and skin cancers.[3] According to the World Health Organization drinking water guidelines, the maximum allowable limit of total chromium is 50 μg/L.[2,5] Therefore, the removal of Cr(VI) from waste effluents is becoming environmentally important.

Several methods have been developed to treat wastewater containing heavy metal ions, including precipitation, sorption, coagulation, ion exchange, solvent extraction, membrane separation, reverse osmosis, and electrochemical treatment.[2,5] Among these methods, sorption is popular because of its simplicity and high efficiency.[2] Many sorbents have been tested for heavy metal ion removal from aqueous solutions,[2,5,6] such as activated carbon, zeolites, minerals (clays), biopolymers, and agro-based and industrial wastes.

Recently, a class of anionic clays known as layered double hydroxides (LDHs) or hydrotalcite-like compounds has attracted considerable attention as a promising sorbent, in view of both performance and cost.[7,8] LDHs can be represented by the general chemical formula $[M^{II}_{1-x}M^{III}_{x}(OH)_2]^{x+}[(A^{n-})_{x/n}\cdot mH_2O]^{x-}$, where M^{II} and M^{III} are di- and trivalent metal cations, respectively, A^{n-} is the interlayer anion (or gallery anion) of charge n, x is the molar ratio of $M^{III}/(M^{II}+M^{III})$, and m is the molar amount of the co-intercalated water per formula

weight of the compound. The structure of LDHs is based on positively charged brucite-like sheets, and the structural positive charges are compensated by exchangeable anions in the interlayer spaces. Owing to the features of high structural positive charge density, large surface area, high anion-exchange capacity, and flexible interlayer space, LDHs exhibit excellent ability to capture organic and inorganic anions. A lot of work has been carried out on the use of LDHs and their calcined products (LDOs) in the removal of various water contaminants.[7-10] Among the previous work, Al-based LDHs such as Mg–Al and Zn–Al are the most widely used,[11-18] owing to the fact that the presence of Al commonly makes LDHs a highly crystalline phase that has high sorption performance for some pollutants.[13,19-22] However, the presence of Al may have serious consequences when using these materials in drinking water treatment. Al exposure is believed to be a potential risk factor for the development or acceleration of Alzheimer's disease in human beings.[11,12] Therefore, Fe-based LDHs or LDHs with complete or partial Fe substitution for Al, such as Mg–Fe or Mg–Al–Fe, have been widely studied as promising candidates for drinking water treatment.[11,12,19-24] The influence of the substitution of Fe for Al in LDHs on their removal performance for pollutants has been investigated.[19-22,25,26] It was found that Al-enriched LDHs exhibit higher removal efficiencies than Fe-enriched LDHs for phosphate,[19] borate,[20] and (4-chloro-2-methylphenoxy) acetic acid contaminants[21] from aqueous solution. In contrast, for the removal of phosphate[25] and NO_3^-[26] from seawater, Al-enriched LDHs have been found to have lower efficiencies than Fe-enriched LDHs. Triantafyllidis et al.[22] investigated the effect of Fe content in Mg–Al–Fe LDHs and LDOs on the sorption capacity for phosphate from aqueous solution. They found that an increase in Fe content led to a decrease in the sorption efficiency of LDHs, while the opposite result was observed for LDOs. Xiao et al.[10] investigated the removal of Cr(VI) by Mg–Al and Mg–Al–Fe LDOs from aqueous solution, and found that the substitution of Fe for Al in the LDOs was favorable for Cr(VI) sorption. These previous reports have revealed that

the nature of the precursor metals in LDHs can significantly influence the sorption of guest oxyanions. However, the influence of the Fe content of Mg–Al–Fe LDHs on their removal efficiency of Cr(VI) has not been reported. In addition, the influence mechanism of Fe content in LDHs on their removal performance for pollutants is not clear.[10]

The most common method to synthesize LDHs is coprecipitation from a mixed metal salt solution.[7,27] However, a significant disadvantage of this conventional method is the production of large amounts of waste.[28,29] A facile and environmentally friendly method to synthesize LDHs is of great practical interest. The mechanochemical method has attracted considerable attention owing to its simplicity and solvent-free feature, and various LDHs have been synthesized using the mechanochemical route.[28,30-34] However, the sorption performance of the resulting LDHs for pollutants from wastewater has not been investigated.

In this study, Mg–Al–Fe LDHs with a constant $Mg^{2+}/(Fe^{3+}+Al^{3+})$ molar ratio but varying Fe^{3+}/Al^{3+} molar ratios were prepared using the mechanochemical method, and the removal efficiency of the prepared LDHs for Cr(VI) from aqueous solution was investigated. The objectives of this work were (i) to investigate the influence of the Fe content of LDHs on the Cr(VI) removal efficiency, and (ii) to evaluate the technical feasibility of using the mechanochemical method to synthesize LDH sorbents.

2. Experimental

2.1. Sorbents

Five Mg–Al–Fe LDH samples were used as sorbents in this study. These LDHs had the same $Mg^{2+}/(Al^{3+}+Fe^{3+})$ molar ratio of 3/1, but different $Fe^{3+}/(Al^{3+}+Fe^{3+})$ molar ratios (R_{Fe}) of 0, 1/3, 1/2, 2/3, or 1. The LDH samples were synthesized using the mechanochemical method via a two-step milling process. Details of the synthetic tests have been described in our previous work.[35,36] In a typical procedure, a mixture of 5.80 g (0.100 mol) $Mg(OH)_2$ and 1.30

g (0.017 mol) $Al(OH)_3$ was milled for 1 h under ambient conditions, and then milled with 6.87 g (0.017 mol) $Fe(NO_3)_3 \cdot 9H_2O$ for a further 5 h, gaining the $LDH_{1/2}$ sample. It is needed to note that a special case is the synthesis of the LDH_0 and LDH_1 samples. For LDH_0 sample, $Mg(NO_3)_2 \cdot 6H_2O$ instead of $Fe(NO_3)_3 \cdot 9H_2O$ was used in the second milling step. For LDH_1 sample, $Mg(OH)_2$ instead of $Al(OH)_3$ was used in the first milling step. The mill used was a planetary ball mill (QM3STC, Nanjing Nanda Instrument Plant, Nanjing, China) with four stainless-steel mill pots (500 cm^3 inner volume) and 10 mm diameter steel-balls. The mill speed was constant at 450 rpm with a ball/mixture mass ratio of approximately 49.

The LDH samples with R_{Fe} values of 0, 1/3, 1/2, 2/3 and 1 (Table S1 in the ESI) are denoted as LDH_0, $LDH_{1/3}$, $LDH_{1/2}$, $LDH_{2/3}$ and LDH_1, respectively. These LDH samples showed irregular aggregate particles,[36] similar to the reported literature.[31] The specific surface area (A_s), average pore size (D_p) and pore volume (V_p) of these sorbents were determined using the N_2 adsorption method (Fig. S1 in the ESI), and the results are summarized in Table 1.

Table 1 Specific surface area, average pore size and pore volume of LDHs

Samples	A_s (m^2 g^{-1})	D_p (nm)	V_p (cm^3 g^{-1})
LDH_0	6.41	2.19	0.024
$LDH_{1/3}$	6.48	3.84	0.017
$LDH_{1/2}$	6.61	2.19	0.034
$LDH_{2/3}$	5.34	2.74	0.012
LDH_1	6.20	2.46	0.018

2.2 Characterization

Powder X-ray diffraction (XRD) patterns of the samples were recorded on a D/max-rA diffractometer (Bruker AXS, Co., Ltd, Germany) with CuKα radiation (λ = 1.5418 Å) at 40 kV and 40 mA in the 2θ range 10–70° with a scanning rate of 10 °/min. Fourier transform infrared

(FT-IR) spectra of the samples were collected using KBr pellets on a Vector-22 FT-IR spectrometer (Bruker AXS, Co., Ltd, Germany) in reflectance mode in the range 400–4000 cm^{-1} with a resolution of 2 cm^{-1}. The X-ray photoelectron spectroscopy (XPS) measurements were performed on a Phi 5300 ESCA system (Perkin-Elmer, USA). The spectra were excited by Mg Kα (1253.6 eV) radiation (operated at 200 W) of a twin anode in constant analyzer energy mode with a pass energy of 30 eV. All of the binding energies were referenced to the C 1s peak at 284.8 eV of the surface adventitious carbon.

2.3 Sorption experiments

The sorption experiments were performed by a batch technique at pH 5.0 and 25.0±0.5 °C. Solutions of Cr(VI) with various concentrations (0–1500 $mg \cdot L^{-1}$) were prepared by dissolving $K_2Cr_2O_7$ in aqueous solutions containing 0.010 $mol \cdot L^{-1}$ $NaNO_3$. The pH values of the solutions were adjusted to 5.0 with 6 $mol \cdot L^{-1}$ HCl and 1 $mol \cdot L^{-1}$ NaOH. Known masses (0.100 g) of the LDHs were mixed with 100 mL of the Cr(VI) solutions in polyethylene centrifuge tubes. The centrifuge tubes were shaken by a thermostatic water bath shaker (Jiangsu Medical Instrument Factory, China) for a given contact time (t) at 25.0±0.5 °C. During this period, the pH values of the systems were adjusted to keep them constant. The suspensions were then filtered through a 0.45 μm membrane, and the Cr(VI) concentrations remaining in the filtrates were determined at 540 nm using a SP-1105 UV-vis spectrometer (Shanghai Spectrum Instruments Co., Ltd, China). The sorption amount (Γ_t) was determined by the difference between the initial and the residual concentrations of Cr(VI):

$$\Gamma_t = (C_0 - C_t)/C_s \qquad (1)$$

where Γ_t ($mg \cdot g^{-1}$) is the sorption amount at time t, C_0 ($mg \cdot L^{-1}$) and C_t ($mg \cdot L^{-1}$) are the initial and the remaining concentrations at time t, respectively, and C_s (g/L) is the sorbent dosage.

Sorption kinetic tests showed that t = 10 h was required to reach equilibrium. To ensure sorption equilibrium, t = 24 h was selected in the equilibrium sorption tests. The equilibrium

sorption amount (Γ_e) was determined from the difference between the initial concentration (C_0) and the equilibrium concentration (C_e). Each test run was performed in triplicate, and the final values were the average of the three measurements. The relative error was less than 6%.

3. Results and discussion

3.1. Sorption kinetics

Fig. 1 shows the effect of contact time on Cr(VI) sorption on the LDHs with C_0 = 100 mg/L. The Γ_t significantly increased within the first 2 h. There was then a slow increase in sorption until equilibrium was reached. The necessary time to reach equilibrium was about 10 h. A contact time of 24 h was chosen to determine Γ_e to ensure sorption equilibrium.

It is well known that the sorption kinetics at solid–liquid interfaces is usually described by pseudo-first-order or pseudo-second-order kinetic models. The two kinetic models can be expressed, respectively, as

$$\Gamma_t = \Gamma_e(1 - e^{-k_1 t}) \quad (2)$$

$$\Gamma_t = \frac{\Gamma_e^2 k_2 t}{1 + \Gamma_e k_2 t} \quad (3)$$

where k_1 (1/h) and k_2 (g/(mg·h)) are the rate constants of pseudo-first-order and pseudo-second-order kinetics, respectively. We used the two kinetic models to analyze the experimental data by a nonlinear regression method (Fig. 1, and Fig. S2 in the ESI), and the best-fit parameters, k_1, k_2, and correlation coefficient (R^2) are summarized in Table 2. The R^2 values obtained from the pseudo-second-order model fitting for various LDHs were significantly higher than those obtained from the pseudo-first-order model fitting, indicating the sorption processes are better described by the pseudo-second-order model than the pseudo-first-order model. Similar results have been reported for Cr(VI) removal in the literature.[4,7,18] Furthermore, with increasing R_{Fe}, k_2 initially increased and then decreased, with

a maximum value at R_{Fe} = 1/2 ($LDH_{1/2}$). In addition, the Γ_e values obtained at C_0 = 100 mg/L increased with increasing R_{Fe}, indicating that replacement of Al by Fe in the LDHs favors sorption of Cr(VI), which was further confirmed by the sorption isotherm results.

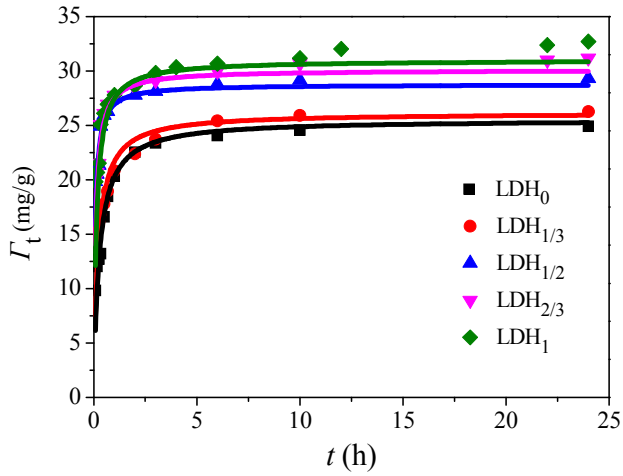

Fig. 1 Kinetics of Cr(VI) sorption on the Mg–Al–Fe LDH samples at C_0 = 100 mg/L. The dots represent the experimental data and the lines represent the pseudo-second-order kinetic model fits.

Table 2 Kinetic model parameters for Cr(VI) adsorption onto Mg-Al-Fe LDHs at C_0 = 100 mg/L

Sample	Γ_e (mg/g)	Pseudo-first-order		Pseudo-second-order	
		k_1 (h^{-1})	R^2	k_2 (g/(mg·h))	R^2
LDH_0	24.92	1.707	0.6014	0.088	0.9646
$LDH_{1/3}$	26.27	3.586	0.1588	0.170	0.9985
$LDH_{1/2}$	29.32	7.709	0.3985	0.404	0.9817
$LDH_{2/3}$	31.18	6.313	0.3496	0.246	0.9668
LDH_1	32.72	5.279	0.2969	0.153	0.9491

3.2. Sorption isotherms

The sorption isotherms of Cr(VI) on the various LDHs are shown in Fig. 2. All of the isotherms were L-type,[15,20] which is consistent with previous studies.[4,13,15,18] L-type isotherms are commonly described using the Langmuir and Freundlich isotherms. The Langmuir model

was developed based on thermodynamic equilibrium theory, while the Freundlich model was originally an empirical equation. However, it was found that the Freundlich equation could be thermodynamically derived assuming that:[37] (*i*) the sorption sites of the sorbent have different sorption energies and (*ii*) sorption of the sorbate on sites with the same energy level obeys the Langmuir equation. That is, the Freundlich isotherm is a thermodynamic model for heterogeneous sorption surfaces.[18]

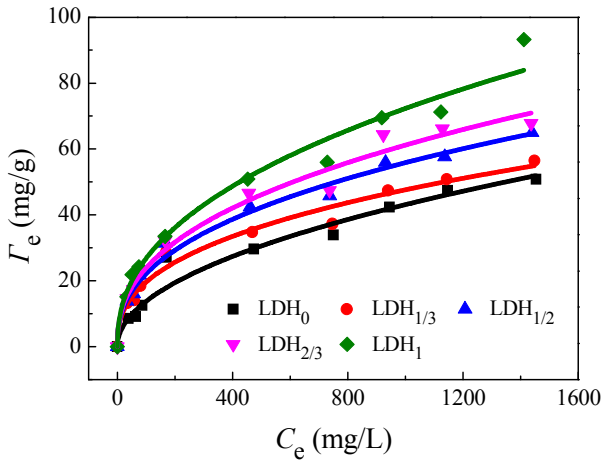

Fig. 2 Sorption isotherms of Cr(VI) on Mg–Al–Fe LDHs. The dots represent the experimental data and the lines represent the Freundlich model fits.

Table 3 Isotherm parameters for Cr(VI) sorption on Mg-Al-Fe LDHs.

Sample	Langmuir isotherm				Freundlich isotherm		
	Γ_m		K_L	R^2	K_F	n_F	R^2
	(mg·g^{-1})	(mg·m^{-2})	(L·g^{-1})		($L^{n_F}mg^{-n_F}$)		
LDH$_0$	56.02	8.74	0.0043	0.9488	1.404	0.496	0.9644
LDH$_{1/3}$	58.45	9.02	0.0064	0.9440	3.327	0.385	0.9809
LDH$_{1/2}$	66.18	10.01	0.0062	0.9668	3.486	0.402	0.9899
LDH$_{2/3}$	73.91	13.84	0.0066	0.9562	3.644	0.408	0.9806
LDH$_1$	89.29	14.40	0.0049	0.9246	3.683	0.431	0.9784

The Langmuir and Freundlich isotherms can be expressed, respectively, as

$$\Gamma_e = \frac{K_L \Gamma_m C_e}{1 + K_L C_e} \quad (4)$$

$$\Gamma_e = K_F C_e^{n_F} \quad (5)$$

where Γ_m (mg/g) is the monolayer saturated sorption amount, K_L (L/mg) is the Langmuir equilibrium constant, and K_F ($L^{n_F} mg^{-n_F}$) and n_F are the Freundlich constants. The sorption data for the LDHs were analyzed with the Langmuir and Freundlich isotherms by a nonlinear regression method (Fig. 2, and Fig. S3 in the ESI). The best-fit values of the model parameters (Γ_m, K_L, K_F, and n_F), as well as R^2, are listed in Table 3. All of the model plots had high R^2 values, suggesting that both the Langmuir and Freundlich isotherms can be used to describe the sorption isotherms of Cr(VI) on the LDHs. Owing to the R^2 values obtained from the Freundlich isotherm fitting for various LDHs were higher than those obtained from the Langmuir isotherm fitting, the sorption equilibriums are better described by the Freundlich isotherm than the Langmuir isotherm. With increasing Fe content of the LDHs, the Γ_m value significantly increased, which is consistent with previous reports on the removal of phosphate[25] and NO_3^-[26] from seawater. This result suggests that the substitution of Fe for Al in the LDHs can increase the affinity of the resulting LDHs for Cr(VI) oxyanions. The reason for this is not clear, although it may be related to the higher electronegativity of Fe (1.83) than Al (1.61). It should be noted that, in contrast to our result, a decrease in sorption with increasing Fe content has been observed in previous work, which included phosphate,[19-22] borate,[20] and (4-chloro-2-methylphenoxy) acetic acid sorbates.[21] In fact, the effects of A_s and D_p of sorbents on sorption should be considered when studying the effect of LDH precursor metals. This is because the sorption capacity of a sorbent is simultaneously determined by many factors, such as the nature of its constituents, crystal structure, and morphology, as well as A_s and D_p. In our case, the A_s and D_p values of the LDH samples are very similar. Thus, the

result that the substitution of Fe for Al influences Cr(VI) sorption can be attributed to the difference in the nature of Fe and Al. Based on the experimental data of Triantafyllidis et al.[22], the sorption of phosphate on LDHs per unit area (mg/m^2) increases with increasing Fe content when considering the effect of A_s of the sorbents on the sorption, which agrees with our result. Xiao et al.[10] reported the substitution of Fe for Al in LDO was favorable for Cr(VI) sorption, but they did not provide the A_s data of their samples.

Furthermore, the Γ_m values of the five LDHs studied in this work are in the range 56.0–89.3 mg/g (8.74–14.40 mg/m^2), which are comparable with previously reported results (about 17–112 mg/g) for LDHs (excluding commercial products) synthesized using coprecipitation or hydrothermal methods[4,7,13,15] when considering the different experimental conditions and different solution matrices being tested in the different studies. These results indicate that the mechanochemical method can be used to synthesize LDH sorbents.

3.3. Sorption mechanism

There are two possible mechanisms for Cr(VI) sorption on LDHs:[4,13,16] (*i*) anion exchange between Cr(VI) oxyanions and interlayer anions of LDHs (or intercalation of Cr(VI) oxyanions into LDH gallery via anion exchange), and (*ii*) surface complexation between Cr(VI) oxyanions and hydroxyl groups of LDH (inner and outer) surfaces. The intercalation (or anion exchange) process may be schematically represented as

$$LDH^{x+}(NO_3^-, CO_3^{2-}) + {}^-O–\{Cr(VI)\}–O^- \rightarrow LDH^{x+}({}^-O–\{Cr(VI)\}–O^-) + NO_3^- + CO_3^{2-}$$

The surface complexation may occur though the chemical and physical complex between Cr(VI) anions and protonated hydroxyl groups of the LDH surfaces, which can be represented, respectively, as

$$Sur–OH_2^+ + {}^-O–\{Cr(VI)\}–O^- \rightleftharpoons Sur–O–\{Cr(VI)\}–O^- + H_2O$$

$$Sur–OH_2^+ + {}^-O–\{Cr(VI)\}–O^- \rightleftharpoons Sur–OH_2^+\cdots{}^-O–\{Cr(VI)\}–O^-$$

In the above expressions, ${}^-O–\{Cr(VI)\}–O^-$ represents the Cr(VI) oxyanions, $Sur–OH_2^+$

represents the protonated hydroxyl groups of the LDH surfaces, and "⋯" represents electrostatic binding. It is no doubt that the intercalation and the surface complexation should simultaneously occur in the Cr(VI) sorption.[4,13,16] Unfortunately, we cannot distinguish the relative ratio of Cr(VI) sorption amounts between the intercalation and the surface complexation according to our information available.

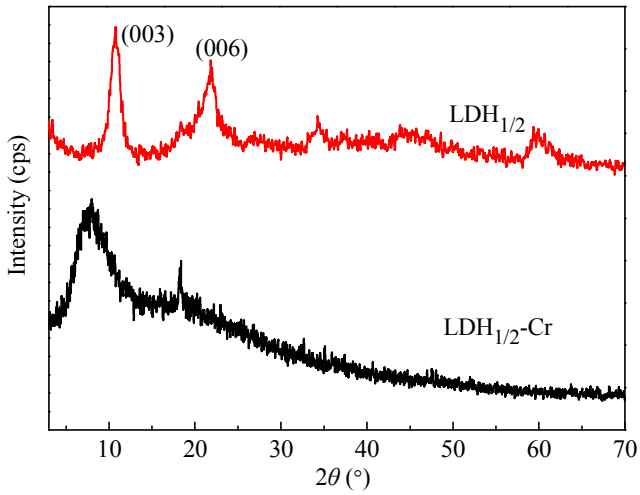

Fig. 3 XRD patterns of $LDH_{1/2}$ and $LDH_{1/2}$-Cr samples.

To check the existence of the intercalation (or anion exchange) process, the XRD patterns of $LDH_{1/2}$ before and after Cr(VI) sorption were determined, as shown in Fig. 3. The Cr(VI)-loaded $LDH_{1/2}$ ($LDH_{1/2}$-Cr) sample was prepared at C_0 = 500 mg/L. The pristine $LDH_{1/2}$ sample exhibited the characteristic diffraction peaks of hydrotalcite (JCPDS card No. 51-1528), indicating that it has the hydrotalcite structure. The d_{003} value is the interlayer spacing (*d*-spacing) of the layered materials. The *d*-spacing of $LDH_{1/2}$ was 0.79 nm, which is lower than the d_{003} value (0.89 nm) of NO_3-LDHs,[16] but close to that reported in the literature for CO_3-LDHs.[20] This result indicates that the interlayer anions of the $LDH_{1/2}$ sample are mainly CO_3^{2-}, resulting from CO_2 sorption from the atmosphere. The $LDH_{1/2}$-Cr sample also clearly showed the (003) diffraction peak, indicating that it remains the hydrocalcite structure. However, the difference in crystallinity between pristine $LDH_{1/2}$ and $LDH_{1/2}$-Cr is significant.

The relatively fine and intense peaks of the pristine $LDH_{1/2}$ sample indicate its good crystalline character, while the wide and ill-defined peaks of the $LDH_{1/2}$-Cr sample indicates a poorly crystalline structure. The lower crystallinity of $LDH_{1/2}$-Cr is probably related to the surface complexation of Cr(VI) on LDHs.[4] Importantly, compared with pristine $LDH_{1/2}$, the (003) basal reflection pattern of $LDH_{1/2}$-Cr obviously shifted to a lower angle, indicating that the *d*-spacing increased. This indicates that Cr(VI) oxyanions were intercalated into the LDH gallery via anion exchange, which is consistent with previous studies.[4,13,16] The *d*-spacing of the $LDH_{1/2}$-Cr sample was 1.12 nm, which is close to the reported value in the literature.[13,16] It is worth noting that a lower d_{003} values (about 0.81–0.86) of Cr(VI)-loaded LDHs have been reported in the literature.[4,13] This difference in the reported d_{003} values results from the different forms of Cr(VI) oxyanions existing in the LDH gallery. The CrO_4^{2-} form usually results in a relatively low d_{003} value, while the $Cr_2O_7^{2-}$ form usually results in a relatively high d_{003} value. In the case of the prepared Cr-$LDH_{1/2}$ sample (C_0 = 500 mg/L and pH = 5), Cr(VI) oxyanions mainly exist as $Cr_2O_7^{2-}$ in solution.[4] As a result, a higher d_{003} value for $LDH_{1/2}$-Cr was observed in this work than in previous studies. As the thickness of a brucite-like layer is about 0.48 nm, the gallery height of $LDH_{1/2}$-Cr is calculated to be 0.64 nm. The length, width, and thickness of $Cr_2O_7^{2-}$ are about 0.55, 0.25, and 0.21 nm, respectively. According to the size of $Cr_2O_7^{2-}$ and the gallery height of $LDH_{1/2}$-Cr, a possible orientation of $Cr_2O_7^{2-}$ anions in the LDHs gallery is proposed in Fig. 4. The $Cr_2O_7^{2-}$ anions are arranged as a monolayer with their long axis approximately perpendicular to the brucite-like layer, where $Cr_2O_7^{2-}$ anions interact with the surface of the LDH layer via electrostatic attraction and hydrogen bonds.

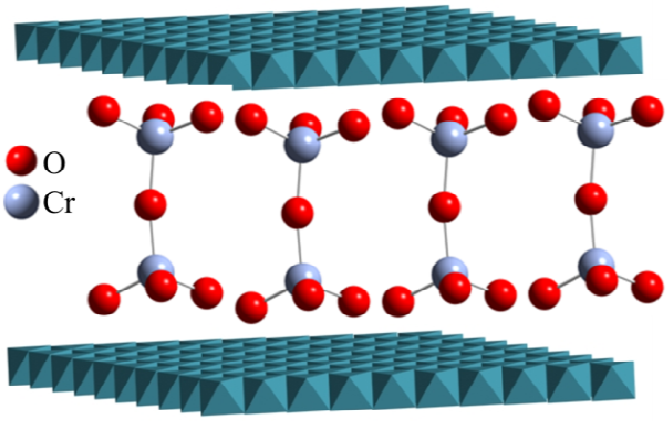

Fig. 4 Proposed structural model of the $LDH_{1/2}$-Cr sample.

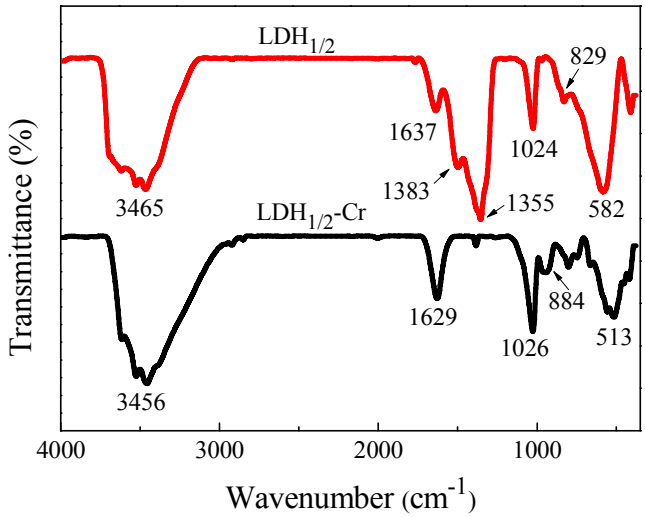

Fig. 5 FT-IR spectra of $LDH_{1/2}$ and $LDH_{1/2}$-Cr.

Fig. 5 shows the FT-IR spectra of the pristine $LDH_{1/2}$ and $LDH_{1/2}$-Cr samples. The FT-IR spectrum of the pristine $LDH_{1/2}$ sample shows all of the characteristic adsorption bands of LDHs materials. The strong and broad band centered at around 3465 cm^{-1} is attributed to the stretching of the hydroxyl groups in the brucite-like layers and interlayer water molecules. The band at 1637 cm^{-1} is the bending vibration of water. The two bands at 1383 and 829 cm^{-1}

are the v_3 and v_2 modes of the interlayer NO_3^-,[20] respectively. The absorption peak at 1355 cm^{-1} is the v_3 mode of CO_3^{2-}.[20] The presence of both the NO_3^- mode at 1383 cm^{-1} and the CO_3^{2-} mode at 1355 cm^{-1} indicates that NO_3^- and CO_3^{2-} coexist in the LDH gallery. In addition, the CO_3^{2-} content is higher than the NO_3^- content because the intensity of the CO_3^{2-} mode is higher than that of the NO_3^- mode, which is consistent with the XRD result (Fig. 3). The other peaks from ~1000 to 400 cm^{-1} can be attributed to the stretching and bending vibrations of M–O and M–OH.[38] After sorption of Cr(VI), the resulting $LDH_{1/2}$-Cr sample shows the characteristic band of chromate at 884 cm^{-1},[4,15,16] which is in agreement with the reported Cr–O stretching mode at 890 cm^{-1} for free chromate ions.[4] The shift of the characteristic band toward a lower frequency (from 890 to 884 cm^{-1}) indicates that the Cr–O bond in the $LDH_{1/2}$-Cr sample is weaker than in free chromate ions, which possibly arises from (*i*) the hydrogen bonding between $Cr_2O_7^{2-}$ and interlayer water molecules or layer hydroxyl groups, and (*ii*) the electrostatic interaction between $Cr_2O_7^{2-}$ and the LDH layers.[16] The hydrogen bonding between the $Cr_2O_7^{2-}$ ions and interlayer water is confirmed by the downshift of the water bending mode before and after Cr(VI) sorption from 1637 to 1629 cm^{-1}. Furthermore, the characteristic peaks of both NO_3^- and CO_3^{2-} almost disappeared in the spectrum of the $LDH_{1/2}$-Cr sample, indicating that these interlayer anions were completely replaced by $Cr_2O_7^{2-}$ ions in solution. This exchangeability of CO_3^{2-} by other anions such as NO_3^- and Cl^- under acidic conditions previously reported.[39,40]

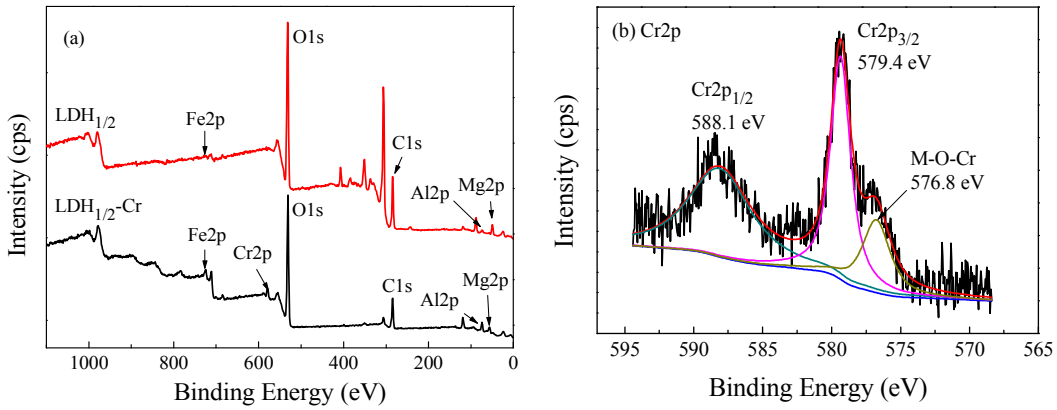

Fig. 6 (a) Survey XPS spectra of $LDH_{1/2}$ and $LDH_{1/2}$-Cr and (b) HR-XPS spectrum of Cr 2p.

Investigation on sorption driving force is helpful to understand the mechanism of sorption. The driving force of Cr(VI) sorption on LDHs possibly includes physical binding (or electrostatic attraction) and chemical binding. To investigate the binding mechanism of Cr(VI) on the LDHs, the XPS spectra of the LDHs before and after Cr(VI) sorption were analyzed. Fig. 6 shows the XPS spectra of the pristine $LDH_{1/2}$ and $LDH_{1/2}$-Cr samples. In the survey XPS spectrum of the pristine $LDH_{1/2}$ sample, the peaks of Fe 2p, O 1s, Al 2p, and Mg 2p are clearly observed at binding energies (E_B) of 713.5, 532.2, 74.5, and 50.4 eV, respectively, and no Cr 2p peak is present. In the survey XPS spectrum of the $LDH_{1/2}$-Cr sample, the peak of Cr 2p is clearly observed at 579.4 eV, indicating that the Cr(VI) anions are sorbed on the LDHs.[3,18] In addition, the peaks of Fe 2p, O 1s, Al 2p, and Mg 2p for the $LDH_{1/2}$-Cr sample were observed at 711.8, 532.3, 74.2, and 56.2 eV, respectively. Comparing with $LDH_{1/2}$, the adsorption of Cr(VI) led to a decrease in the E_B values of Fe 2p and O 1s by 1.7 and 0.9 eV, a significant increase in the E_B value of Mg 2p by 5.8 eV, and no obvious change in the E_B value of Al 2p (a decrease of only 0.3 eV). The dramatic change in the E_B values of Fe 2p and Mg 2p before and after Cr(VI) sorption suggests that some Cr(VI) anions are chemically bonded to O atoms bonded to the metal atoms. The different changes in the E_B values of the

different metal elements induced by Cr(VI) sorption can be attributed to their different electronegativities. The electronegativity of Cr (1.66) is lower than those of Fe (1.83) and O (3.44), higher than that of Mg (1.31), and close to that of Al (1.61). The high-resolution XPS (HR-XPS) spectrum of Cr 2p in the $LDH_{1/2}$-Cr sample (Fig. 6b) can provide more information about the binding mechanism. The dominant peak observed at 579.4 eV is attributed to Cr $2p_{3/2}$, and the Cr $2p_{1/2}$ peak appeared at 588.1 eV.[41] The peaks of Cr $2p_{3/2}$ and Cr $2p_{1/2}$ in $K_2Cr_2O_7$ were observed at 579.4 and 588.8 eV, respectively (Fig. S4 in the ESI). The close E_B values of the Cr 2p peaks in $LDH_{1/2}$-Cr and $K_2Cr_2O_7$ suggests the existence of a Cr(VI) physical binding. That is, the dominant peak at 579.4 eV can be assigned to physically sorbed Cr(VI). Moreover, another peak at 576.8 eV was observed in the HR-XPS spectrum of Cr 2p in the $LDH_{1/2}$-Cr sample (Fig. 6b), which can be attributed to the formation of (Mg, Fe, or Al)–O–Cr (chemical complex). That is, the peak can be assigned to chemically sorbed Cr(VI).

Similar results were obtained for the other LDH and LDH-Cr samples (Fig. S5 in the ESI), and the XPS data are summarized in Table 4. All of the LDH-Cr samples were prepared at C_0 = 500 mg/L. With an increase in the Fe content in the LDHs, there was an increasing trend in the E_B values of O 1s, Al 2p, and Mg 2p, which is because the electronegativity of Fe (1.83) is higher than that of Al (1.61). Moreover, from the HR-XPS spectra of Cr 2p for various LDH-Cr samples (Fig. S6 in the ESI), the area ratios of the peak at 576.8 eV to the peak at 579.4 eV for LDH_0-Cr, $LDH_{1/3}$-Cr, $LDH_{1/2}$-Cr, $LDH_{2/3}$-Cr, and LDH_1-Cr were 12:88, 17:83, 31:69, 37:63, and 40:60, respectively, which shows that the percentage of chemical bonding content in the Cr(VI)-loaded samples increased with increasing R_{Fe}. Moreover, from the relative percentage data of the chemical and physical bonding contents in the Cr(VI)-loaded samples, we can obtained that, under the saturated sorption states, the physical bonding amounts for various samples are very close, being 48.72 $mg \cdot g^{-1}$ with an maximum relative error of < 10%, while the chemical bonding amount dramatically increases from 6.72

mg·g^{-1} to 35.72 mg·g^{-1} with increasing R_{Fe} from 0 to 1. This result suggests that the increase of Fe content leads to enhanced activity of the surface sorption sites. This may be a possible reason of increasing Fe content increasing Cr(VI) sorption.

4. Conclusion

The sorption of Cr(VI) on Mg–Al–Fe LDHs synthesized by the mechanochemical method with varying R_{Fe} was investigated. With increasing R_{Fe}, Γ_m increased, indicating that the substitution of Fe for Al is favorable for Cr(VI) sorption. The sorption process is best described by pseudo-second-order kinetics, and the sorption equilibrium can be well described with the Freundlich isotherm. The Cr(VI) sorption arises from physical binding (or electrostatic attraction) and chemical binding. The increase of R_{Fe} causes the chemical activity of surface sorption sites of the LDHs to increase, resulting in their sorption capacity for Cr(VI) increasing. Mg–Fe LDHs are promising sorbents for treating Cr(VI)-containing wastewater, and the facile and environmentally friendly mechanochemical method can be used to synthesize the LDH sorbents.

Acknowledgment: This research was supported by the National Natural Science Foundation of China (No. 21173135) and the Specialized Research Fund for the Doctoral Program of Higher Education of China (No. 20110131130008).

References

1 R. P. Schwarzenbach, B. I. Escher, K. Fenner, T. B. Hofstetter, C. A. Johnson, U. Von Gunten, B. Wehrli, Science, 2006, **313**, 1072–1077.

2 P. Miretzky, A. F. Cirelli, J. Hazard. Mater. 2010, **180**, 1–19.

3 Z. Ai, Y. Cheng, L. Zhang, J. Qiu, Environ. Sci. Technol. 2008, **42**, 6955–6960.

4 Y. Li, B. Gao, T. Wu, D. Sun, X. Li, B. Wang, F. Lu, Water Res. 2009, **43**, 3067–3075.

5 M. Owlad, M. K. Aroua, W. A. W. Daud, S. Baroutian, Water, Air, Soil Pollut. 2009, **200**, 59–77.

6 S. E. Bailey, T. J. Olin, R. M. Bricka, D. D. Adrian, Water Res. 1999, **33**, 2469–2479.

7 K. H. Goh, T. T. Lim, Z. Dong, Water Res. 2008, **42**, 1343–1368.

8 X. Liang, Y. Zang, Y. Xu, X. Tan, W. Hou, L. Wang, Y. Sun, Colloids Surf. A, 2013, **433**, 122–131.

9 F. Li, X. Duan, Struct Bond. 2006, **119**, 193–223.

10 L. Xiao, W. Ma, M. Han, Z. Cheng, J. Hazard. Mater. 2011, **186**, 690–698.

11 Y. Seida, Y. Nakano, Y. Nakamura, Water Res. 2001, **35**, 2341–2346.

12 J. Das, B. S. Patra, N. Baliarsingh, K. M. Parida, J. Colloid Interface Sci. 2007, **316**, 216–223.

13 R. L. Goswamee, P. Sengupta, K. G. Bhattacharyya, D. K. Dutta, Appl. Clay Sci. 1998, **13**, 21–34.

14 N. Lazaridis, D. Asouhidou, Water Res. 2003, **37**, 2875–2882.

15 E. Álvarez-Ayuso, H. W. Nugteren, Water Res. 2005, **39**, 2535–2542.

16 Y. B. Zang, W. G. Hou, W. X. Wang, Acta Chim. Sin. 2007, **65**, 773–778.

17 S. Q. Zhang, W. G. Hou, Chin. J. Chem. 2007, **25**, 1455–1460.

18 Y. Chen, Y. F. Song, Ind. Eng. Chem. Res. 2013, **52**, 4436–4442.

19 J. Das, B. S. Patra, N. Baliarsingh, K. M. Parida, Appl. Clay Sci. 2006, **32**, 252–260.

20 O. P. Ferreira, S. G. de Moraes, N. Durán, L. Cornejo, O. L. Alves, Chemosphere, 2006, **62**, 80–88.

21 F. Bruna, R. Celis, I. Pavlovic, C. Barriga, J. Cornejo, M. A. Ulibarri, J. Hazard. Mater. 2009, **168**, 1476–1481.

22 K. S. Triantafyllidis, E. N. Peleka, V. G. Komvokis, P. P. Mavros, J. Colloid Interface Sci. 2010, **342**, 427–436.

23 J. Das, D. Das, G. P. Dash, K. M. Parida, J. Colloid Interface Sci.2002, **251**, 26–32.

24 X. Liang, W. Hou, J. Xu, Chin. J. Chem. 2009, **27**, 1981–1988.

25 R. Chitrakar, S. Tezuka, A. Sonoda, K. Sakane, K. Ooi, T. Hirotsu, J. Colloid Interface Sci. 2006, **297**, 426–433.

26 S. Tezuka, R. Chitrakar, A. Sonoda, K. Ooi, T. Tomida, Green Chem. 2004, **6**, 104–109.

27 J. He, M. Wei, B. Li, Y. Kang, D. G. Evans, X. Duan, Struct Bond. 2006, **119**, 89–119.

28 V. Khusnutdinov, V. Isupov, Inorg. Mater. 2008, **44**, 263–267.

29 A. N. Ay, B. Zümreoglu-Karan, L. Mafra, Z. Anorg. Allg. Chem. 2009, **635**, 1470–1475.

30 R. Chitrakar, S. Tezuka, A. Sonoda, K. Sakane, K. Ooi, T. Hirotsu, Chem. Lett. 2007, **36**, 446–447.

31 W. Tongamp, Q. Zhang, F. Saito, J. Mater. Sci. 2007, **42**, 9210–9215.

32 W. Tongamp, Q. Zhang, F. Saito, Powder Technol. 2008, **185**, 43–48.

33 T. Iwasaki, K. Shimizu, H. Nakamura, S. Watano, Mater. Lett. 2012, **68**, 406–408.

34 F. Zhang, N. Du, R. Zhang, and W. Hou, Powder Technol. 2012, **228**, 250–253.

35 F. Zhang, N. Du, S. Song, J. Liu, W. Hou, J. Solid State Chem. 2013, **206**, 45–50.

36 F. Zhang, N. Du, H. Li, J. Liu, W. Hou, Solid State Sci. 2014, **32**, 41–47.

37 C. Sheindorf, M. Rebhun, M. Sheintuch, J. Colloid Interface Sci. 1981, **79**, 136–142.

38 M. K. Titulaer, J. B. H. Jansen, J. W. Geus, Clays Clay Miner. 1994, **42**, 249–258.

39 N. Iyi, K. Okamoto, Y. Kaneko, T. Matsumoto, Chem. Lett. 2005, **34**, 932–933.

40 Z. Liu, R. Ma, Y. Ebina, N. Iyi, K. Takada, T. Sasaki, Langmuir 2007, **23**, 861–867.

41 L. Chen, B. Y. He, S. He, T. J. Wang, C. L. Su, Y. Jin, Powder Technol. 2012, **227**, 3–8.